0273-2289/02/98-100/0341/$13.75

Characterization of Heterologous and Native Enzyme Activity Profiles in Metabolically Engineered *Zymomonas mobilis* Strains During Batch Fermentation of Glucose and Xylose Mixtures

Qiang Gao,[1] Min Zhang,[2] James D. McMillan,[2] and Dhinakar S. Kompala*,[1]

[1]Department of Chemical Engineering, University of Colorado, Boulder, CO 80309-0424, E-mail: kompala@colorado.edu; and [2]Biotechnology Division for Fuels and Chemicals, National Renewable Energy Laboratory, Golden, CO 80401-3933

Abstract

Zymomonas mobilis has been metabolically engineered to broaden its substrate utilization range to include D-xylose and L-arabinose. Both genomically integrated and plasmid-bearing *Z. mobilis* strains that are capable of fermenting the pentose D-xylose have been created by incorporating four genes: two genes encoding xylose utilization metabolic enzymes (*xylA/xylB*) and two genes encoding pentose phosphate pathway enzymes (*talB/tktA*). We have characterized the activities of the four newly introduced enzymes for xylose metabolism, along with those of three native glycolytic enzymes, in two different xylose-fermenting *Z. mobilis* strains. These strains were grown on glucose–xylose mixtures in computer-controlled fermentors. Samples were collected and analyzed to determine extracellular metabolite concentrations as well as the activities of several intracellular enzymes in the xylose and glucose uptake and catabolism pathways. These measurements provide new insights on the possible bottlenecks in the engineered metabolic pathways and suggest methods for further improving the efficiency of xylose fermentation.

Index Entries: Recombinant *Zymomonas mobilis*; xylose fermentation; enzyme analysis; ethanol; byproducts.

*Author to whom all correspondence and reprint requests should be addressed.

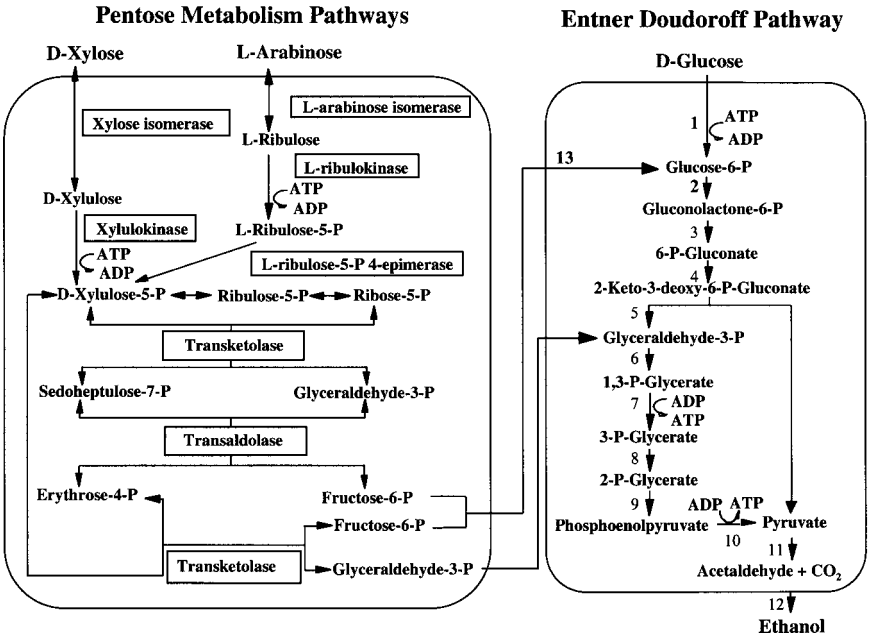

Fig. 1. Postulated reaction pathways required for *Zymomonas* pentose fermentation. The left side of the diagram shows the putative pentose metabolism pathways and the cloned enzymes (shown in rectangular boxes) whose presence confers pentose fermentation capability. The right side of the diagram shows the native Entner Doudoroff (ED) hexose utilization pathway. The numbered enzymes in the ED pathway are: 1, glycokinase; 2, glucose-6-phosphate dehydrogenase; 3, 6-phospho gluconolactonase; 4, 6-phosphogluconate dehydratase; 5, 2-keto-3-deoxy-6-phospho gluconate [KDPG] aldolase; 6, glyceraldehyde-3-phosphate dehydrogenase; 7, 3-phosphoglycerate kinase; 8, phosphoglycerate mutase; 9, enolase; 10, pyruvate kinase; 11, pyruvate decarboxylase; 12, alcohol dehydrogenase; and 13, phosphoglucose isomerase.

Introduction

There is interest in producing fuel ethanol from renewable biomass to reduce petroleum dependence and mitigate net production of carbon dioxide. Although the bacterium *Zymomonas mobilis* is ideal for fermentative fuel ethanol production *(1)*, the narrow carbon source range of native *Z. mobilis*—glucose, fructose, and sucrose—has limited its application for fermenting xylose-containing biomass sugar hydrolyzates. Metabolic engineering has been used to develop *Z. mobilis* strains exhibiting broader substrate utilization ranges *(2,3)*. Strains that are capable of fermenting D-xylose or L-arabinose have been constructed. Figure 1 illustrates the putative metabolic pathways for xylose and arabinose assimilation in these strains. Genomically integrated and plasmid-bearing *Z. mobilis* strains that are capable of fermenting the pentose D-xylose have been created by incorporating four genes: two genes encoding xylose utilization metabolic enzymes (*xylA/xylB*) and two genes encoding pentose phosphate pathway

enzymes (*tal/tktA*). Metabolically engineered strains expressing these four genes exhibit good ethanol production on glucose–xylose mixtures.

Materials and Methods

Microorganisms

Two recombinant *Z. mobilis* strains, both derived from *Z. mobilis* ATCC 39676, were used in this study:

1. Strain C25: a genomically integrated strain in which the *xylA/xylB* and *talB/tktA* genes are present in two distinct synthetic operons *(4)*.
2. Adapted strain 39676/pZB4L: a variant of plasmid pZB4L-bearing strain 39676/pZB4L that grows faster on xylose *(5)*. The plasmid contains the *xylA/xylB* and *talB/tktA* genes in separate synthetic operons as well as a gene encoding for tetracycline resistance (*tet*). The adapted variant was isolated following long-term continuous culture on hardwood hemicellulose hydrolyzate.

Culture Media

Seed cultures of both *Z. mobilis* strains were prepared using a two-stage process. Frozen stock cultures were first revived by inoculating a single cryovial into 10 mL of nutrient medium containing the following components (amounts are in g/L): glucose, 20; yeast extract, 10; and KH_2PO_4, 2. After 21 h of static incubation at 30°C, 10 mL of the revived culture was transferred to a 500 mL bottle containing: glucose, 20 g/L; xylose, 20 g/L; yeast extract, 10 g/L; and KH_2PO_4, 2 g/L. After 17.5 h of static incubation at 30°C, cells in this culture were harvested and concentrated by centrifugation (3370*g*, 10 min, 4°C). Fermentors were inoculated with concentrated inoculum to achieve an initial optical density of 0.20–0.25 absorbance units at 600 nm (approximately 0.07 g/L dry cell mass). Fermentations were carried out using a nutrient medium similar to those used for seed production, except containing higher levels of glucose and xylose (40 ± 1 g/L each). All media were autoclaved for batch fermentation studies by sterilizing at 121°C for 45 min. For the adapted plasmid-bearing strain, tetracycline was added to the autoclaved media at a concentration at 20 mg/L just before inoculation to ensure selection pressure to maintain the pZB4L plasmid.

Fermentation

Fermentations were conducted for 48 h in two 3-L BIOFLO 3000 fermentors (New Brunswick Scientific, Edison, NJ) using a working volume of 2.5 L. They were controlled at a temperature of 30°C, a pH of 5.5 (by automatic addition of 3 *N* KOH), and an agitation rate of 150 rpm. Samples were collected periodically for analysis of cell mass, sugar, ethanol, and by-product concentrations. The volume of sample was adjusted as required based on cell mass concentration to obtain an amount of cell

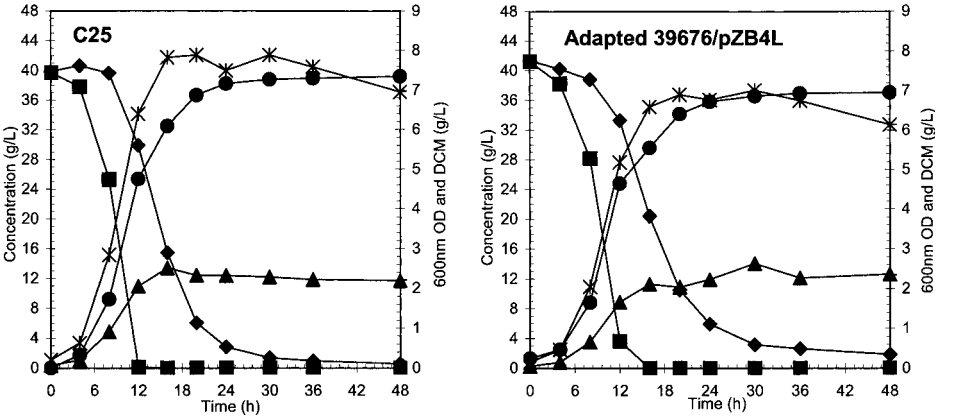

Fig. 2. Batch fermentation profiles. ■, glucose; ◆, xylose; ●, ethanol; ▲, dry cell mass; ✳, OD600nm.

mass equivalent to 25 mL of fermentation broth at a turbidity or optical density (OD) at 600 nm of 1.0. Clarified sample filtrates were obtained by filtering 1.5 mL of sample supernatant produced by centrifuging at 3370*g* for 10 min and 4°C using a Beckman GS-15R centrifuge (Beckman, Palo Alto, CA). Sample filtrates were washed once with sonication buffer (10 m*M* Tris, pH 7.6, 10 m*M* $MgCl_2$) supplemented with 1 m*M* DTT and stored at –20°C prior to analysis. The turbidity of whole broth samples was measured and used to estimated cell mass concentration (based on a previously developed calibration).

Preparation of Cell-Free Extracts

Cell-free extracts for enzyme assays were prepared as follows: 0.5 mL of 20-fold concentrated cell suspension in sonication buffer were sonicated for 45 s twice at 62% duty cycle and an output control of 2 using a Branson model 450 sonifier (Branson ultrasonics, Danbury, CT). The sonication samples were then centrifuged at 17,350*g* and 4°C for 45 min using a Beckman GS-15R centrifuge. The supernatant was recovered and then the sample was recentrifuged at 17,350*g* and 4°C for another 20 min. The resulting supernatant was used as cell-free extracts.

Analytical methods

The concentrations of glucose, xylose, ethanol, and by-products (xylitol, lactate, glycerol, and acetate) were determined from filtered sample supernatants using an HP 1090 HPLC equipped with a refractive index detector (Hewlett-Packard, Palo Alto, CA). Component separation was achieved using a Bio-Rad HPX-87H hydrogen ion resin column (Bio-Rad Labs, Richmond, CA) running at a temperature of 65°C and using 0.01 *N* H_2SO_4 as the mobile phase. Mixed component standards containing glucose, xylose, and ethanol were periodically run to verify calibration accuracy. The fermentations profile results shown in Fig. 2 are based on single time point determinations.

Enzyme Assays

Cell-free extracts obtained from time course samples were assayed for heterologous and selected native enzyme activities. All of the seven enzyme activities were assayed at 340 nm and 30°C in a final volume of 0.5 mL using a Beckman DU-640 spectrophotometer (Beckman, Fullerton, CA). Xylose isomerase (EC 5.3.1.5) was measured in a mixture containing 0.128 m*M* NADH, 50 m*M* xylose, 10 m*M* $MgSO_4$, 1 m*M* triethanolamine, 0.5 U sorbitol dehydrogenase, and 50 µL CFE. Xylulokinase (EC 2.7.1.17) was assayed as Eliasson et al. described *(6)*. The assay buffer contained 0.2 m*M* NADH, 50 m*M* Tris-HCl (pH 7.5), 2 m*M* $MgCl_2$, 2 m*M* ATP, 0.2 m*M* phosphoenolpyruvate, 8.5 m*M* ATP, 2.5 U pyruvate kinase, 2.5 U lactate dehydrogenase, and 10–50 µL CFE. Transaldolase (EC 2.2.1.2) was measured according to De Graaf et al. *(7)*. Transketolase (EC 2.2.1.1) was determined according to Sprenger et al. *(8)*. Phosphoglucose isomerase (EC 5.3.1.9), glucokinase (EC 2.7.1.2), and glucose-6-phosphate dehydrogenase (EC 1.1.1.49) were assayed using the method reported by Algar and Scopes *(9)*. Enzyme assays were performed in on cell-free extracts in duplicate or triplicate. The error bars in Figs. 3 and 4 represent ±1 standard deviation about the mean when assays were run in triplicate or ±1 deviation about the average when assays were run in duplicate.

Calculations

All calculations assume constant volume or neglect the (minor) impact of volume changes. Metabolic ethanol yields were calculated based on the amount of total sugar (glucose + xylose) consumed. Process ethanol yields were calculated based on the amount of sugars initially present. Maximum theoretical ethanol yields of 0.51 g ethanol per g sugar (glucose or xylose) were assumed (see Table 1). Volumetric sugar uptake rates were calculated directly based on the change in sugar concentration over the time interval of interest. Specific sugar uptake rates, i.e., uptake rates per gram of cell mass, were calculated using the average cell concentration over the time interval of interest.

Results

Batch Fermentation Performance

Batch fermentations were carried out on mixtures of glucose and xylose (each initially present at a concentration of 40 g/L) to compare the performance and enzyme activity levels of *Z. mobilis* strains C25 (genomic integrant) and adapted 39676/pZB4L (plasmid-bearing variant).

Cell Growth

As shown in Table 2 and Fig.2, *Z. mobilis* strain C25 grew to a modestly higher cell mass concentration than adapted 39676/pZB4L. Maximum cell mass concentrations, which were reached by both strains in 16–30 h, were 2.5 and 2.6 g dry cell mass per liter (g DCM/L) for strains C25 and adapted 39676/pZB4L, respectively.

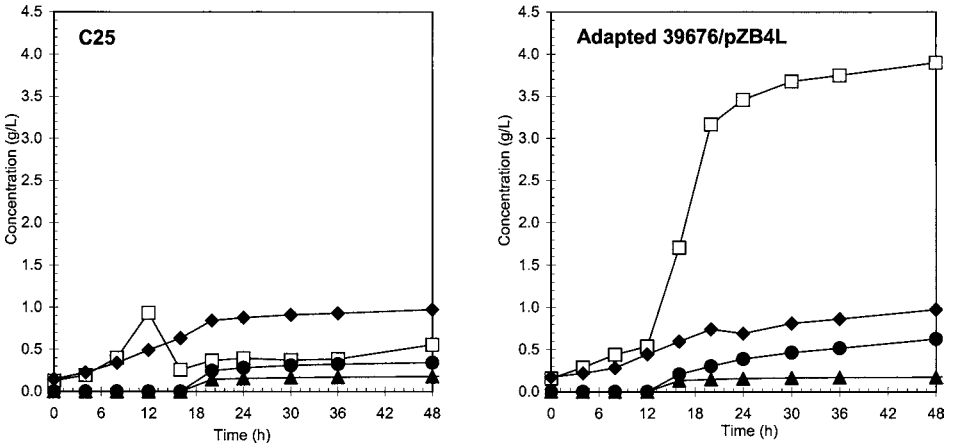

Fig. 3. Byproduct formation profiles. □, xylitol; ◆, lactate; ▲, glycerol; ●, acetate.

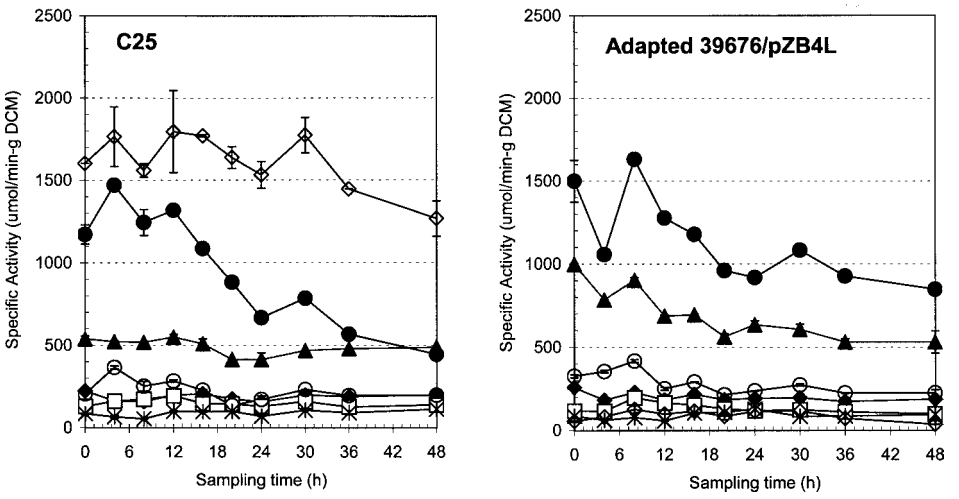

Fig. 4. Dynamic enzyme profiles during batch fermentation for each strain. ◆, PGI; □, GK; ▲, GPD; ✱, XI; ◇, XK; ●, TAL; ⊖, TKT.

Table 1
Stoichiometry of Glucose and Xylose Fermentation to Ethanol

glucose + ADP + P_i → 2 ethanol + 2 CO_2 + ATP
3 xylose + 3 ADP + 3 P_i → 5 ethanol + 5 CO_2 + 3 ATP
Theoretical ethanol yield = 0.51 g ethanol/g sugar (glucose or xylose)

Table 2
Fermentation Time Course Data

Time (h)	Glucose (g/L)	Xylose (g/L)	OD or Cell mass (g/L, dry basis)	Turbidity (@600 nm)	Ethanol (g/L)	Process Yield[a] (%)	Metabolic Yield[b] (%)	Xylitol (g/L)	Lactate (g/L)	Glycerol (g/L)	Acetate (g/L)
Strain: C25											
0	39.71	39.85	0.065	0.20	0.00	0.0	0.0	0.13	0.15	0.00	0.00
4	37.81	40.62	0.20	0.63	1.74	4.3	298.9	0.20	0.23	0.00	0.00
8	25.31	39.62	0.91	2.84	9.23	22.7	123.6	0.40	0.34	0.00	0.00
12	0.15	29.88	2.06	6.40	25.35	62.5	100.4	0.93	0.49	0.00	0.00
16	0.00	15.45	2.51	7.82	32.50	80.1	99.4	0.26	0.63	0.00	0.00
20	0.00	6.06	2.33	7.88	36.63	83.9	97.7	0.37	0.84	0.14	0.25
24	0.00	2.83	2.32	7.49	38.18	94.1	97.6	0.40	0.88	0.16	0.28
30	0.00	1.37	2.29	7.88	38.75	95.5	97.2	0.37	0.91	0.17	0.31
36	0.00	0.96	2.22	7.58	38.90	95.9	97.0	0.39	0.93	0.17	0.33
48	0.00	0.56	2.19	6.95	39.18	96.5	97.2	0.56	0.97	0.18	0.34
60	0.00	0.48	2.41	7.24	39.15	96.5	97.1	0.41	1.01	0.22	0.41
72	0.00	0.39	2.06	6.79	38.99	96.1	96.6	0.40	0.98	0.22	0.44
Strain: Adapted 39676/pZB4L											
0	41.24	41.36	0.048	0.15	1.30	0.0	0.0	0.16	0.17	0.00	0.00
4	38.25	40.23	0.15	0.46	2.51	2.9	57.7	0.29	0.22	0.00	0.00
8	28.16	38.79	0.66	2.05	8.82	17.9	94.2	0.44	0.28	0.00	0.00
12	3.62	33.27	1.66	5.18	24.79	55.8	100.8	0.54	0.45	0.00	0.00
16	0.00	20.39	2.11	6.58	29.59	67.2	89.2	1.71	0.60	0.13	0.21
20	0.00	10.51	2.04	6.89	34.14	78.0	89.3	3.17	0.74	0.15	0.31
24	0.00	5.94	2.23	6.76	35.81	81.9	88.3	3.46	0.69	0.16	0.39
30	0.00	3.13	2.63	7.00	36.56	83.7	87.0	3.68	0.81	0.17	0.47
36	0.00	2.61	2.27	6.74	36.95	84.6	87.4	3.75	0.86	0.17	0.52
48	0.00	1.85	2.36	6.14	37.09	85.0	86.9	3.90	0.97	0.17	0.63
60	0.00	1.36	2.09	6.22	36.59	83.8	85.2	4.07	1.08	0.26	0.81
72	0.00	1.07	2.11	6.50	36.58	83.8	84.9	4.04	1.04	0.27	0.86

[a]Based on available sugars.
[b]Based on consumed sugars.

(Continued)

Table 2 *(Continued)*
Fermentation Time Course Data

Strain: C25, Fermentor 1: #5

Time (h)	Glucose (g/L)	Xylose (g/L)	Dry cell mass (g/L)	OD or Turbidity (@600 nm)	Ethanol (g/L)	Xylitol (g/L)	Lactate (g/L)	Glycerol (g/L)	Acetate (g/L)
	40.79	40.94		0.022	0.00	0.13	0.16	0.00	0.00
0	39.71	39.85	0.065	0.202	0.00	0.13	0.15	0.00	0.00
4	37.81	40.62	0.20	0.626	1.74	0.20	0.23	0.00	0.00
8	25.31	39.62	0.91	2.84	9.23	0.40	0.34	0.00	0.00
12	0.15	29.88	2.06	6.40	25.35	0.93	0.49	0.00	0.00
16	0.00	15.45	2.51	7.82	32.50	0.26	0.63	0.00	0.00
20	0.00	6.06	2.33	7.88	36.63	0.37	0.84	0.14	0.25
24	0.00	2.83	2.32	7.49	38.18	0.40	0.88	0.16	0.28
30	0.00	1.37	2.29	7.88	38.75	0.37	0.91	0.17	0.31
36	0.00	0.96	2.22	7.58	38.90	0.39	0.93	0.17	0.33
48	0.00	0.56	2.19	6.95	39.18	0.56	0.97	0.18	0.34

Strain: Adapted 39676/pZB4L, Fermentor 2: #6

Time (h)	Glucose (g/L)	Xylose (g/L)	Dry cell mass (g/L)	OD or Turbidity (@600 nm)	Ethanol (g/L)	Xylitol (g/L)	Lactate (g/L)	Glycerol (g/L)	Acetate (g/L)
	41.46	41.46		0.03	1.28	0.16	0.18	0.00	0.00
0	41.24	41.36	0.048	0.15	1.30	0.16	0.17	0.00	0.00
4	38.25	40.23	0.15	0.46	2.51	0.29	0.22	0.00	0.00
8	28.16	38.79	0.66	2.05	8.82	0.44	0.28	0.00	0.00
12	3.62	33.27	1.66	5.18	24.79	0.54	0.45	0.00	0.00
16	0.00	20.39	2.11	6.58	29.59	1.71	0.60	0.13	0.21
20	0.00	10.51	2.04	6.89	34.14	3.17	0.74	0.15	0.31
24	0.00	5.94	2.23	6.76	35.81	3.46	0.69	0.16	0.39
30	0.00	3.13	2.63	7.00	36.56	3.68	0.81	0.17	0.47
36	0.00	2.61	2.27	6.74	36.95	3.75	0.86	0.17	0.52
48	0.00	1.85	2.36	6.14	37.09	3.90	0.97	0.17	0.63

Sugar Uptake

As shown in Table 3 (A,B) and in Fig. 2, the highest sugar uptake rates by both strains were obtained for glucose and occurred from 0 to 12 h; this was the most rapid phase of ethanol production and cell growth. During this period, *Z. mobilis* strains C25 and adapted 39676/pZB4L exhibited respective maximum specific glucose uptake rates of 5.6 and 7.6 g/g-h (4–8 h and 0–4 h averages, respectively) and overall average specific glucose uptake rates of 3.1 and 3.7 g/g-h (0–12 h averages).

Table 2 *(Continued)*
Fermentation Time Course Data

Interval Volumetric Glucose uptake (g/L·h)	Interval Specific Glucose uptake (g/g-h)	0- final time Specific Glucose uptake (g/g-h)	Interval Volumetric Xylose uptake (g/L·h)	Interval Specific Xylose uptake (g/g-h)	0- final time Specific Xylose uptake (g/g-h)	Interval Specific Ethanolproduction (g/L·h)	Interval Specific Ethanolproduction (g/g-h)	0- final time Specific Ethanolproduction (g/g-h)
Strain: C25, Fermentor 1: #5								
0.48	3.58	3.58	−0.19	−1.44	−1.44	0.43	3.26	3.26
3.12	5.61	3.68	0.25	0.45	0.061	1.87	3.36	2.36
6.29	4.24	3.11	2.43	1.64	0.78	4.03	2.72	1.99
0.04	0.02	1.93	3.61	1.58	1.18	1.79	0.78	1.58
0.00	0.00	1.66	2.35	0.97	1.41	1.03	0.43	1.53
0.00	0.00	1.38	0.81	0.35	1.29	0.39	0.17	1.33
0.00	0.00	1.13	0.24	0.11	1.09	0.095	0.041	1.10
0.00	0.00	0.97	0.068	0.030	0.95	0.025	0.011	0.95
0.00	0.00	0.73	0.034	0.015	0.73	0.023	0.011	0.72
Strain: Adapted 39676/pZB4L, Fermentor 2: #6								
0.75	7.59	7.59	0.28	2.87	2.87	0.30	3.08	3.08
2.52	6.25	4.63	0.36	0.89	0.91	1.58	3.91	2.66
6.14	5.28	3.66	1.38	1.19	0.79	3.99	3.44	2.29
0.90	0.48	2.38	3.22	1.70	1.21	1.20	0.64	1.64
0.00	0.00	1.98	2.47	1.19	1.48	1.14	0.55	1.57
0.00	0.00	1.51	1.14	0.53	1.30	0.42	0.20	1.26
0.00	0.00	1.03	0.47	0.19	0.95	0.13	0.052	0.88
0.00	0.00	0.99	0.086	0.035	0.93	0.065	0.026	0.85
0.00	0.00	0.71	0.064	0.028	0.68	0.011	0.005	0.62

Table 3 (C,D) shows the rates of xylose utilization by the two strains. Maximum specific xylose uptake rates were highest for *Z. mobilis* strain C25 for the 12–16 h time period, and highest for the adapted 39676/pZB4L strain over the 0–4 h time period. *Z. mobilis* strains C25 and adapted 39676/pZB4L exhibited maximum specific xylose uptake rates during these intervals of 1.6 g/g-h (12–16 h) and 2.9 g/g-h (0–4 h), respectively. The overall average specific xylose uptake rates for these two strains were similar after 20 h at 1.4 and 1.5 g/g-h (0–20 h average), respectively. The most rapid rate of xylose utilization rate was achieved by the adapted *Z. mobilis* 39676/pZB4L strain.

Table 3
Glucose, Xylose Uptake and Ethanol Production Rates

Table 3 A Glucose uptake (g/g-h)

time interval (h)	0–4	4–8	8–12	12–16	16–20	20–24	24–30	30–36	36–48
C25	3.6	5.6	4.2	0.0	0.0	–0.0	0.0	0.0	0.0
39676 pZB4L adapted	7.6	6.2	5.3	0.5	0.0	0.0	0.0	0.0	0.0

Table 3 B Glucose uptake (g/g-h)

time interval (h)	0–4	0–8	0–12	0–16	0–20	0–24	0–30	0–36	0–48
C25	3.6	3.7	3.1	1.9	1.7	1.4	1.1	1.0	0.7
39676 pZB4L adapted	7.6	4.6	3.7	2.4	2.0	1.5	1.0	1.0	0.7

Table 3 C Xylose uptake (g/g-h)

time interval (h)	0–4	4–8	8–12	12–16	16–20	20–24	24–30	30–36	36–48
C25	–1.4	0.5	1.6	1.6	1.0	0.3	0.1	0.0	0.0
39676 pZB4L adapted	2.9	0.9	1.2	1.7	1.2	0.5	0.2	0.0	0.0

Table 3 D Xylose uptake (g/g-h)

time interval (h)	0–4	0–8	0–12	0–16	0–20	0–24	0–30	0–36	0–48
C25	–1.4	0.1	0.8	1.2	1.4	1.3	1.1	0.9	0.7
39676 pZB4L adapted	2.9	0.9	0.8	1.2	1.5	1.3	1.0	0.9	0.7

Table 3 E Ethanol production (g/g-h)

time interval (h)	0–4	4–8	8–12	12–16	16–20	20–24	24–30	30–36	36–48
C25	3.3	3.4	2.7	0.8	0.4	0.2	0.0	0.0	0.0
39676 pZB4L adapted	3.1	3.9	3.4	0.6	0.5	0.2	0.1	0.0	0.0

Table 3 F Ethanol production (g/g-h)

time interval (h)	0–4	0–8	0–12	0–16	0–20	0–24	0–30	0–36	0–48
C25	3.3	2.4	2.0	1.6	1.5	1.3	1.1	0.9	0.7
39676 pZB4L adapted	3.1	2.7	2.3	1.6	1.6	1.3	0.9	0.9	0.6

Ethanol Production

As shown in Table 2 and Fig. 2, *Z. mobilis* strains C25 and adapted 39676/pZB4L produced maximum ethanol concentrations at 48 h of 39.2 and 37.1 g/L, respectively. Table 2 shows that *Z. mobilis* strain C25 achieved a final metabolic ethanol yield (yield based on consumed sugar) of 97% of theoretical, whereas the adapted 39676/pZB4L strain only achieved a final metabolic ethanol yield of 87% of theoretical. As Table 3 (E,F) show, specific ethanol productivities were highest in the 0–12 h time period for both strains. During this period, *Z. mobilis* strains C25 and adapted 39676/pZB4L exhibited maximum specific ethanol production rates of 3.4 and 3.9 g/g-h (4–8 h average) or 2.0 and 2.3 g/g-h (0–12 h

average), respectively. As these figures and tables show, *Z. mobilis* strain C25 achieved modestly faster ethanol production than the adapted 39676/pZB4L strain.

Byproduct Formation

HPLC analysis of fermentation broth samples detected four minor by-products: acetate, lactate, glycerol, and xylitol. As Fig. 3 illustrates, production levels of all by-products other than xylitol was very low, generally below 1 g/L. The presence of acetate has been reported previously to detrimentally affect fermentation performance by xylose-utilizing *Z. mobilis* strains, decreasing the rates of xylose uptake and ethanol production *(5,10)*. In this study, however, only very small amounts of by-product acetate were produced. The low levels of acetate production are unlikely to have significantly decreased the rates of xylose uptake or ethanol production rates during the fermentations.

Figure 3 shows that xylitol was a significant by-product of ethanol fermentation for the plasmid-bearing 39676/pZB4L strain. The accumulation of xylitol correlates positively with ethanol production, but correlates negatively with the ethanol production rate, i.e., the higher the amount of xylitol accumulation, the lower the rate of ethanol production. However, this observation could be made for any by-product that accumulates, since ethanol production generally decreases over time in a batch process.

Enzyme Activities

The dynamic enzyme activity trends for the seven enzymes tracked in this study [xylose isomerase (XI), xylulokinase (XK), transaldolase (TAL), transketolase (TKT), phosphoglucose isomerase (PGI), glucokinase (GK), and glucose-6-phosphate dehydrogenase (GPD)] are shown in Figs. 4 and 5. The dynamic profiles for the four foreign enzymes enabling xylose assimilation and metabolism (XI, XK, TAL, and TKT) are generally similar in the two tested strains, with the notable exception of XK. As Figs. 4 and 5 vividly show, XK activity levels in strain C25 are over 10 fold higher than in the adapted 39676/pZB4L strain. Although the differences are markedly less, TKT activity levels are modestly higher in the adapted 39676/pZB4L strain than in the C25 strain.

The dynamic enzyme activity profile results for the three native Entner Doudoroff (ED) pathway enzymes (GK, GPD, and PGI) are also fairly similar in the two tested strains. A possible exception is GPD, which remains throughout the fermentation at somewhat higher activity levels in the adapted 39676/pZB4L strain than in strain C25.

Discussion

The amount of cell mass produced by the two tested strains peaked between 16 and 30 h (Fig. 2). Ethanol production was modestly faster in strain C25 than in the adapted plasmid-bearing strain, but both strains

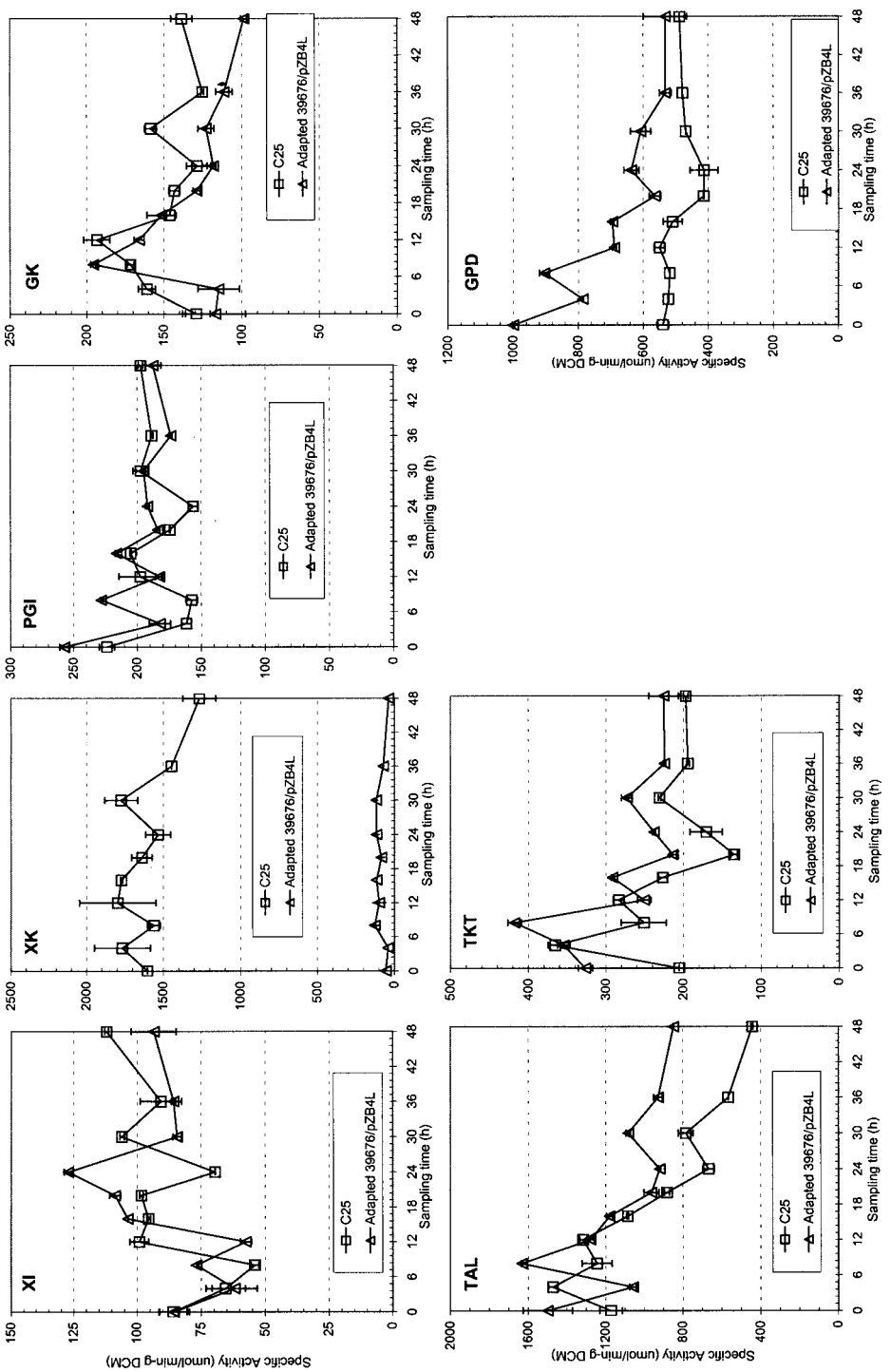

Fig. 5. Comparative activity profiles for each enzyme. □, C25; △, adapted 39676/pZB4L.

continued to produce ethanol, albeit at diminishing rates, up to 48 h (Tables 2 and 3, Fig. 2). Consumption of glucose and xylose peaked within the first 16 h and was substantially completed within 30–36 h; extending the fermentation to 48 h did little to benefit ethanol production and mainly increased the level of by-product formation. The adapted 39676/pZB4L strain exhibited the highest rates of xylose uptake, but estimates of sugar uptake rates were also significantly influenced by the sampling frequency.

The comparative results described here show the powerful potential of using microbial genetics to reduce by-product formation levels in a batch fermentation process. In particular, the use of improved strain construction techniques based on chromosomal integration offers the potential to minimize the activity of undesirable product formation pathways. So far, strain C25 exhibits much more efficient ethanol production characteristics than the plasmid-bearing adapted 39676/pZB4L strain (Fig. 2). This occurs in spite of the fact that both of these strains contain the same synthetic xylose utilization and pentose phosphate metabolism operons. The differences in gene transcription and protein expression between these two strains need to be better understood so that strains with further improved characteristics can be constructed. And performance must be assessed over a wider range of glucose and xylose concentrations to understand comparative strain behavior over a broader range of operating conditions, including those of greatest interest to industry.

Since glucose uptake ended before 16 h for both of the strains tested, our preliminary results suggest that the carbon flux of glucose and glucose intermediates through the ED pathway is not influenced by the presence of the four heterologous xylose utilization genes, whether they are integrated into the strain's chromosome or carried on an extrachromosomal plasmid. This hypothesis is supported but not proven by the results of the dynamic enzyme activity profiles, which generally do not show dramatic changes in enzyme activity levels as the fermentation switches from using glucose as the main substrate to using xylose. We plan to use *in situ* NMR to measure the concentrations (and fluxes) of postulated intracellular phosphorylated sugar intermediates to test this hypothesis *(7,11)*.

The specific activity of XK was over 10-fold higher in the C25 strain than in the adapted 39676/pZB4L strain. Since specific glucose and xylose uptake rates, as well as specific ethanol production rates, were very similar in both tested strains, XK is not considered to be the primary bottleneck enzyme constraining the rate of xylose fermentation. The dramatically higher activity of this enzyme in C25 strain might be due to a mutation in the enzyme's structure or, and less likely, as a consequence of a higher level of expression in the genomically integrated strain.

The specific activities of TAL and TKT were similar in both tested strains. Close examination of these results shows that after about 12–16 h the specific activities of these two enzymes appear to begin to decrease. From this point forward, modest differences in the levels of these two enzymes are observed between the two strains, with the better ethanol-

producing strain, strain C25, expressing lower specific activities than the adapted strain. Based on the fact that better ethanol production occurs in the strain that expresses lower amounts of these enzymes, neither TAL nor TKT activities appear to be substantially limiting the rate of xylose fermentation.

The specific activity of XI was similar in both tested strains and the absolute activity levels of this enzyme were the lowest among all seven enzymes tested. These preliminary results therefore identify XI as a probable bottleneck enzyme in the xylose uptake and metabolism pathway, i.e., an enzyme whose activity likely constrains the rate of xylose fermentation. This observation is different from that obtained previously by de Graaf et al. *(7)*, perhaps as a consequence of these authors having used a different methodology to assay XK activity *(6,7)*. Regardless, the speculation that XI is a rate limiting or bottleneck enzyme still needs to be verified by more rigorously determining the biochemical characteristics of each of the four foreign enzymes introduced into these strains to catalyze xylose uptake and pentose phosphate metabolism.

Sugar uptake rates and ethanol production rates were not markedly affected regardless of whether the four foreign genes were plasmid-borne or introduced via chromosomal integration. However, the activity of GPD, as well as the amounts of minor byproducts, especially xylitol, were measurably higher in the adapted 39676/pZB4L strain than in the genomically integrated C25 strain.

Conclusions

Both of the xylose-fermenting *Z. mobilis* strains tested, genomically integrated strain C25 and plasmid-bearing adapted 39676/pZB4L, exhibited good conversion performance at 30°C and pH 5.5 on mixtures of glucose and xylose (40 g/L each), achieving ethanol yields between 87 and 97% of the theoretical maximum. Strain C25 utilized xylose more completely, produced modestly higher maximum cell mass and ethanol concentrations, and generated the smallest amount of by-products of the two xylose-fermenting strains tested. The adapted 39676/pZB4L strain exhibited higher initial rates of xylose uptake but converted the mixed sugars to ethanol at about a 10% lower conversion efficiency than strain C25. The adapted 39676/pZB4L strain also produced higher levels of by-products than strain C25, producing substantially higher amounts of xylitol and modestly higher amounts of acetate.

The dynamic profiles for xylose isomerase, transaldolase, transketolase, phosphoglucose isomerase, and glucokinase showed approximately similar specific activities trends for both tested strains. However, glucose-6-phosphate dehydrogenase activities remained higher in the adapted 39676/pZB4L strain than in the C25 strain. In contrast, the specific activities of xylulokinase remained significantly higher in the C25 strain than in the adapted strain. The specific activity levels of xylose isomerase

were similar but quite low in both strains, suggesting that this enzyme might be a bottleneck in the engineered xylose metabolism pathway.

Acknowledgments

This work is funded by the United States Department of Agriculture 99-35505-8685 and the Biochemical Conversion Element of the Office of Fuels Development of the U.S. Department of Energy.

References

1. Lawford, H. G. (1988), *Appl. Biochem. Biotechol.* **17,** 203–219.
2. Zhang, M., Eddy, C., Deana, K., Finkelstein, M., and Picataggio, S. (1995), *Science* **267,** 240–243.
3. Deanda, K., Zhang, M., Eddy, C., and Picataggio, S. (1996), *Appl. Environ. Microbiol.* **62,** 4465–4470.
4. Zhang, M. and Chou, Y.-C. (2000), Stable *Zymomonas mobilis* xylose and arabinose-fermenting strains, US patent pending.
5. Lawford, H. G., Rousseau, J. D., Mohagheghi, A., and McMillan J. D. (1999), *Appl. Biochem. Biotechnol.* **77–79,** 191–204.
6. Eliasson, A., Boles, E., Johansson, B., Österberg, M., Thevelein, J, M., Spencer-Martins, I., Juhnke, H., and Hahn-Hägerdal, B. (2000), *Appl. Microbiol. Biotechnol.* **53,** 376–382.
7. de Graaf, A. A., Striegel, K., Wittig, R. M., Laufer, B., Schmidt, G., Wiechert, W., Sprenger, G. A., and Sahm, H. (1999), *Arch. Microbiol.* **171,** 371–385.
8. Sprenger, G. A., Schörken, U., Sprenger, G., and Sahm, H. (1995), *Eur. J. Biochem.* **230,** 525–532.
9. Algar, E. M. and Scopes, R. K. (1985), *J. Biotechnol.* **2,** 275–287.
10. Joachimsthal, E. L. and Rogers, P. L. (2000), *Appl. Biochem. Biotechnol.* **84–86,** 343–356.
11. Kim, I. S., Barrow, K. D., and Rogers, P. L. (2000), *Appl. Biochem. Biotechnol.* **84–86,** 357–370.